Journal of Zhejiang University-SCIENCE A (Applied Physics & Engineering)
ISSN 1673-565X (Print); ISSN 1862-1775 (Online)
www.zju.edu.cn/jzus; www.springerlink.com
E-mail: jzus@zju.edu.cn

Operating characteristics of a single-stage Stirling-type pulse tube cryocooler with high cooling power at liquid nitrogen temperatures*

Jiu-ce SUN[1,2,3], Marc DIETRICH[2,3], Li-min QIU[†‡1], Guenter THUMMES[†‡2,3]

([1]*Institute of Refrigeration and Cryogenics, Zhejiang University, Hangzhou 310027, China*)

([2]*Institute of Applied Physics, University of Giessen, D-35392 Giessen, Germany*)

([3]*TransMIT-Centre for Adaptive Cryotechnology and Sensors, D-35392 Giessen, Germany*)

[†]E-mail: Limin.Qiu@zju.edu.cn; Guenter.Thummes@ap.physik.uni-giessen.de

Received Mar. 24, 2015; Revision accepted June 8, 2015; Crosschecked June 16, 2015

Abstract: The operating characteristics are important for design and optimization of pulse tube cryocoolers, in particular for those with high cooling power, which up to now have been seldom extensively investigated. In this study, the dependence of cooling performance on the charge pressure and operating frequency has been investigated, both numerically and experimentally. A numerical model based on Sage software was established. Experiments were performed on a home-made single-stage high power Stirling-type pulse tube cryocooler (SPTC) working at liquid nitrogen temperatures. The results revealed that each charge pressure corresponds to an optimum frequency with respect to compressor and regenerator efficiency. A lower charge pressure results in a higher cryocooler efficiency, but the delivered maximum pV power is significantly reduced due to the stroke limit of the pistons in the linear compressor. The influence of operating characteristics on the temperature non-uniformity in the regenerator was also investigated. By optimizing the charge pressure and frequency, the minimum no-load temperature was decreased to 46.9 K at 56.5 Hz and 2.0 MPa. A cooling power of 300 W at 71.8 K was measured with an electrical input power of 8.9 kW.

Key words: Stirling-type pulse tube cryocooler (SPTC), High power, Operating characteristics, Temperature non-uniformity
doi:10.1631/jzus.A1500057 **Document code:** A **CLC number:** TB661

1 Introduction

High-power cryocoolers show promise in satisfying the increasing requirements of high temperature superconductor cooling and small-scale gas liquefaction (Gromoll *et al*., 2006; Dietrich *et al*., 2007; 2010; Sun *et al.*, 2009a). The Stirling-type pulse tube cryocooler (SPTC) is one of the best candidates among the regenerative cryocoolers, because of its advantages of compactness, low vibration, high reliability, and high efficiency (Gan *et al*., 2008; Yan *et al.*, 2009). However, scaling up the cooling capacity to hundreds of watts or even kilowatts is still challenging, mainly owing to some stubborn problems, such as flow inhomogeneity, temperature inhomogeneity, and impedance matching between compressor and cold head (Potratz *et al.*, 2008; Sun *et al.*, 2009b).

Different approaches have been presented to improve the performance of high power SPTCs in the past decade. Dietrich *et al*. (2007) designed a single-stage high power SPTC. By use of sandwich type regenerator fillings, where a part of the original stainless screens was replaced by copper or brass screens with higher thermal conductance, the losses from streaming were significantly reduced and the refrigeration temperature was lowered to 34.5 K. Cooling power of 50 W at 45 K and 200 W at 70 K was available with electrical input power of 6.3 kW

‡ Corresponding authors

* Project supported by the National Natural Science Foundation of China (No. 50776076), the Doctoral Fund of the Ministry of Education of China (No. 20110101110022), and the National Funds for Distinguished Young Scientists of China (No. 50825601)

ORCID: Li-min QIU, http://orcid.org/0000-0003-1943-8902; Guenter THUMMES, http://orcid.org/0000-0003-0371-962X

and 8.6 kW, respectively (Dietrich *et al*., 2007). By optimizing the length to diameter ratio of the regenerator and the thickness of the flow straightener, the SPTC developed by Ercolani *et al.* (2008) reached a no-load refrigeration temperature of 39.6 K. A cooling power of 302 W was achieved at 77 K with an input power of 7.5 kW. Imura *et al.* (2008) applied coupled fillings by mixing different mesh stainless steel screens with copper screens in the regenerator in a high capacity SPTC. The no-load temperature was reduced to 37.8 K, and the cooling power was 180 W at 80 K at an input power of 3.8 kW. Hu *et al.* (2014) lengthened the regenerator and pulse tube to avoid possible temperature inhomogeneity in a coaxial SPTC. With 7.6 kW electrical input power, the cryocooler offers more than 520 W cooling power at 80 K corresponding to a relative Carnot efficiency of 18.2%.

Up to now, most research has focused on the optimization of the geometrical parameters including dimensions and regenerator fillings. However, there is little quantitative research to reveal the relationship between operating parameters and cooling performance. The effect of charge pressure in high power SPTCs with double-inlet configuration was theoretically studied and compared to literature data by Ghahremani *et al*. (2011). To our knowledge, no systematic studies on the operating characteristics of high power SPTCs have been reported, which will be necessary for further enhancement of performance.

In this study, a single-stage high power SPTC was employed to investigate the effect of operating parameters, such as the charge pressure and frequency on the cooling performance. Numerical simulations together with the experimental results illustrate the dependence of refrigeration temperature, cooling capacity, and regenerator temperature inhomogeneity on the charge pressure and operating frequency. This should benefit the design and optimization of high power SPTCs.

2 Numerical Sage model

To investigate the dependence of cooling performance, a numerical model was established by use of the software Sage (Gedeon, 1994). Fig. 1 illustrates the SPTC configuration in the Sage model. The SPTC consists of a linear compressor, primary shell-and-tube aftercooler, flow straightener, regenerator, slot cold heat exchanger, pulse tube, warm heat exchanger, and inertance tube with reservoir for phase shifting. The inertance tube was optimized by using three different sections to improve the phase shifting at the cold end of the pulse tube. The explanations of variables in Fig. 1 will be given in Section 3. The dimensions of the main parts of the SPTC are listed in Table 1. For cryocoolers working at high power, a regenerator with large cross-sectional area but small aspect ratio is preferred for hydrodynamic reasons (reduced friction loss along the regenerator). According to the numerical simulation, the diameter and length of the regenerator was selected to be 117 and 49 mm, respectively.

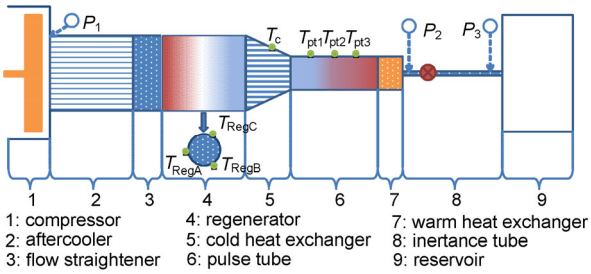

Fig. 1 Schematic of the inline single-stage PTC with linear compressor

Table 1 Dimensions of the main components of the high power single-stage SPTC

Component		Value
Regenerator	Diameter (mm)	117
	Length (mm)	49
Regenerator matrix	Wire diameter (μm)	30
	Porosity	0.65
Pulse tube	Diameter (mm)	45
	Length (mm)	170
Inertance 1	Diameter (mm)	13
	Length (m)	0.62
Inertance 2	Diameter (mm)	15
	Length (m)	1.0
Inertance 3	Diameter (mm)	20
	Length (m)	1.0

3 Experimental setup

Experiments are performed on a single-stage high power SPTC designed and manufactured at the TransMIT-Center for Adaptive Cryotechnology and

Sensors (Giessen, Germany) with the aid of a Sage model (Dietrich *et al*., 2007). The SPTC setup adopts an inline configuration of pulse tube and regenerator, as schematically shown in Fig. 1. The compressor, the aftercooler, and the warm heat exchanger are water-cooled. The commercial linear compressor with dual opposed pistons (QDrive model 42SM-2S297W) has a nominal electrical input power of 10 kW at a maximum acoustic power of about 8 kW. The compressor is equipped with two position sensors along the axial direction of the piston and a pressure sensor (P_1) at the outlet, which enables the measurement of the generated pV power. Two additional pressure sensors (P_2 and P_3) are installed close to the warm heat exchanger and at the inlet to the reservoir. To determine the efficiencies of the compressor and of the cold head, the electrical input power W_{el} is also monitored. Seven calibrated Pt-100 resistance thermometers are installed in the cryocooler. One is located at the cold heat exchanger to measure the refrigeration temperature T_c. As illustrated in Fig. 1, three Pt-100 sensors (T_{RegA}, T_{RegB}, T_{RegC}) are equidistantly mounted on the circumference of the regenerator tube at half of its length in order to measure the azimuthal temperature distribution. Three Pt-100 sensors, labeled as T_{pt1}, T_{pt2}, T_{pt3}, are installed along the pulse tube wall to measure the temperature profile of the pulse tube. The relative measurement error of the Pt-100 thermometers used is only 2.4% at 80 K.

Hybrid regenerator fillings are used to increase the transverse thermal conductance of the regenerator matrix, to reduce the temperature inhomogeneity and the associated losses (Dietrich *et al.*, 2007; Imura *et al.*, 2008). As illustrated in Fig. 2, 400# mesh stainless steel screens were filled in the cold end of the regenerator with a temperature of T_c. The temperature at the warm end of regenerator T_h was equal to the ambient temperature. Theoretical investigations (Dietrich *et al*., 2007) indicate that the maximum temperature non-uniformity will occur in the middle of the regenerator. As a result, the hybrid regenerator fillings with higher thermal conductivity were positioned in the middle of the regenerator. Two matrices are tested: matrix 1 consists of 352# mesh brass screens and 80# mesh copper screens with a proportion of 5:1 in the middle and some 352# mesh brass screens at the warm end of the regenerator together with certain 400# mesh stainless steel screens at the cold end; matrix 2 employs 400# mesh stainless steel screens and 80# mesh copper screens with a proportion of 5:1 in the middle and 400# mesh stainless steel screens at the warm and cold ends (Fig. 2).

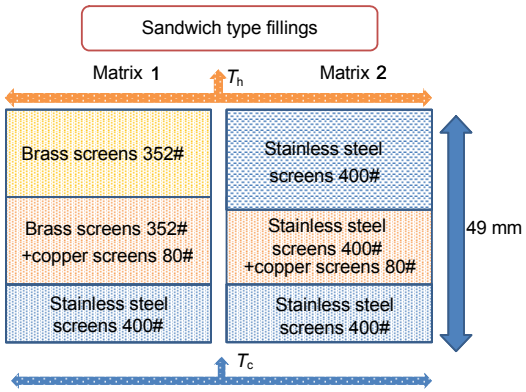

Fig. 2 Schematic of the hybrid regenerator fillings

4 Results and discussion

4.1 Effect of operating frequency

The operating frequency has a significant impact on the performance of the cryocooler. The cryocooler realizes cooling power via two energy transformation processes: electrical-acoustic power conversion occurring in the compressor and acoustic-heat conversion taking place inside the regenerator; both of these are critically affected by the operating frequency as will be discussed below.

Fig. 3 illustrates the measured influence of operating frequency on the compressor working condition. The relationship between the cosine of the phase angle ϕ_{el} between current and voltage, which is a measure for the absorbed power with respect to actual power, and operating frequency is shown in Fig. 3a for different charge pressures with matrix 1. The electrical input power is kept constant at 7.0 kW, and no additional heat load is applied to the cryocooler. Fig. 3a clearly shows the influence of operating frequency on the electrical resonance state of the compressor, which affects the maximum input power that can be delivered by the power supply. Moreover, the electrical resonance frequency decreases with the reduction of charge pressure due to the lower stiffness of the gas spring.

The operating frequency not only influences the electrical impedance of the compressor, but also affects the mechanical impedance that is strongly related to the efficiency of the compressor (defined as generated pV power divided by the electrical input

power). Because of limitations in our measurement system, the phase between the current and the stroke indicating the mechanical resonance of the compressor could not be measured. Instead, Fig. 3b shows the measured variation of the quotient of the generated pV power W_{pV} and the electrical current I, which can be taken as an indicator for mechanical resonance, as function of operating frequency. The operating conditions were the same as those in Fig. 3a. The mechanical response shows a similar dependence on charge pressure as the electrical resonance, except that the resonance frequency is slightly shifted to lower values by 2–3 Hz. The compressor efficiency as function of operating frequency is also shown in Fig. 3c for the same operating conditions as those in Figs. 3a and 3b. A comparison of Figs. 3b and 3c indicates that the compressor efficiency reaches its maximum near the mechanical resonance. Although the compressor efficiency is independent of the electrical reactance (Wakeland, 2000), which determines the electrical resonance, it is better to have the two resonance frequencies close to one another in order to increase the available acoustic power.

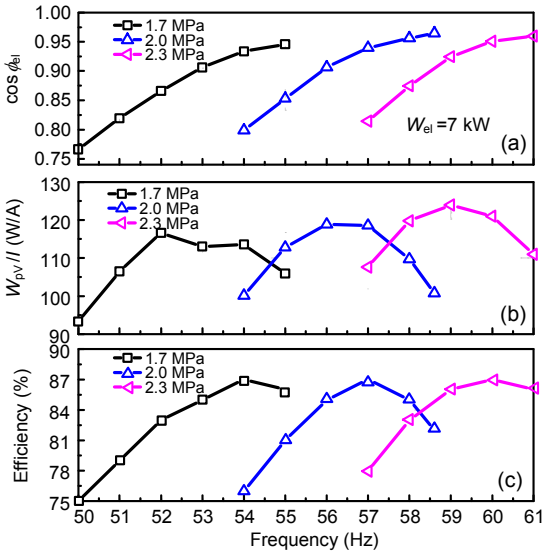

Fig. 3 Measured electrical response (cosϕ_{el}) as function of frequency (a); measured mechanical response (W_{pV}/I) as function of frequency (b); and measured pV power conversion efficiency as function of frequency (c)

The influence of operating frequency on the cryocooler efficiency not only depends on the compressor efficiency, but also on the thermo-acoustic efficiency of the regenerator via the phase shifter network connected to the cooler. The contour graphs in Figs. 4 and 5 show the calculated phase angle between mass flow and pressure wave at the warm and cold ends of the regenerator, respectively. The pV power is kept constant at 7 kW and the refrigeration temperature is fixed to 80 K. As indicated by comparison of Figs. 4 and 5, at a frequency of about 55 Hz, the phase shift between mass flow and pressure wave is roughly +20° at the warm end of the regenerator and near –20° at the cold end.

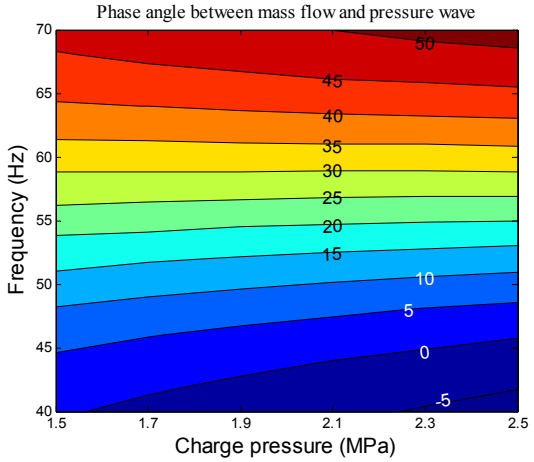

Fig. 4 Calculated phase angle between mass flow and pressure wave at the warm end of the regenerator

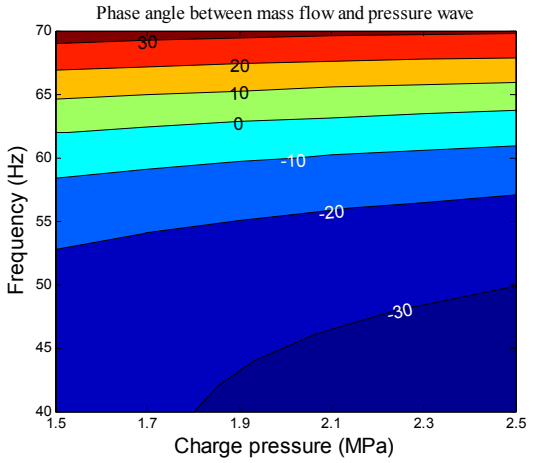

Fig. 5 Calculated phase angle between mass flow and pressure wave at the cold end of the regenerator

This means that at 55 Hz the mass flow is approximately in phase with the pressure wave in the middle of the regenerator; thus the friction loss in the regenerator reaches its minimum at this frequency (Fig. 6). Fig. 7 shows the calculated refrigeration temperature with different thermal loads as function

of frequency. There exists an optimum frequency with respect to the lowest refrigeration temperature. With 400 W of heat load, the optimum frequency is close to 55 Hz, which is in conjunction with the frequency for optimum phase shift in the regenerator (Figs. 4 and 5). In addition, as shown in Fig. 7, the gradients of the curves below and above the optimum frequency are different. When the frequency is higher than the optimum, the refrigeration temperature varies much faster than that below the optimum, which holds for all thermal loads from 0 to 400 W, with the exception that the lowest temperature is shifted slightly towards lower frequencies at higher heat loads, as indicated by the dotted line in Fig. 7. This is mainly because the cold head acoustic impedance changes with temperature. This simulation result suggests that the optimum frequency depends on the refrigeration temperature range; a higher refrigeration temperature requires a lower optimum frequency.

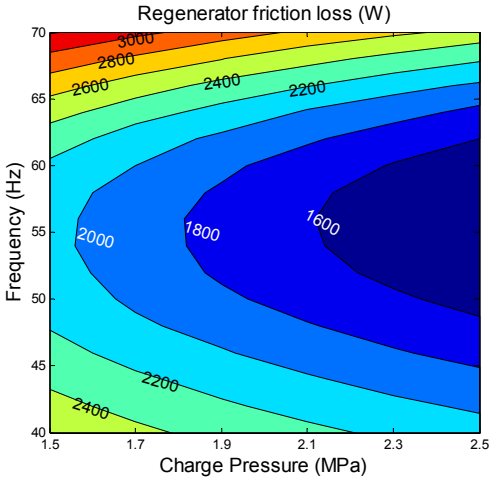

Fig. 6 Calculated regenerator friction loss as function of frequency and charge pressure

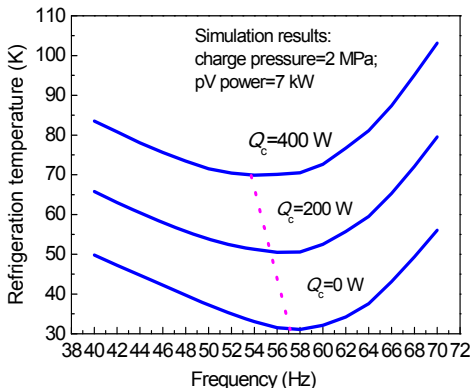

Fig. 7 Calculated refrigeration temperature as function of frequency for different thermal loads

Fig. 8a shows the measured relative Carnot efficiency of the cryocooler (defined as the coefficient of performance COP×(T_h−T_c)/T_c where T_h=284 K and T_c=80 K) and the pV power conversion efficiency as function of frequency for a high charge pressure of 2.38 MPa using matrix 1. The relative Carnot efficiency of the cryocooler was measured in a rather small frequency range around the resonance frequency with a maximum possible electrical input power of 8.9–9.3 kW. Due to the current limit of the linear motors, the pV efficiency as function of frequency was measured with a lower electrical input power of 6 kW.

In addition, the frequency dependence of both electrical ($\cos\phi_{el}$) and mechanical (W_{pV}/I) responses at the same input power of 6 kW are shown in Fig. 8b. Since the mechanical resonance frequency does not vary with input power, the extreme values of the curves in Fig. 8 can be directly compared. The highest relative Carnot efficiency is reached at an operating frequency of 59.5 Hz, which is slightly lower than the optimum operating frequency with the highest W_{pV}/I for the compressor under these conditions, as seen from a comparison with Fig. 8b.

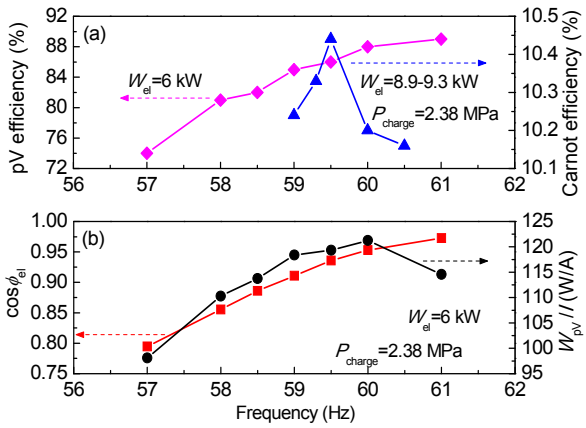

Fig. 8 Measured relative Carnot efficiency, pV power conversion efficiency versus operating frequency (a) and measured electrical and mechanical responses versus operating frequency (b)

This finding is attributed to the fact that at the lower frequency of 55 Hz, the regenerator efficiency reaches its maximum as evaluated from the numerical simulation above (Figs. 4 and 5). Therefore, the optimization of frequency with respect to high efficiency of the cryocooler has to take into account compressor as well as regenerator efficiency.

4.2 Effect of charge pressure

The previous section revealed that besides the operating frequency, the charge pressure also influences the compressor efficiency. In this section we will discuss how the charge pressure affects the cold head. Fig. 9 displays the measured optimum frequency, cooling power at 80 K, no-load temperature, pV power, and relative Carnot efficiency as function of charge pressure with the regenerator filled with matrix 1. For each charge pressure several operating frequencies, which were slightly smaller than the mechanical resonant frequency, have been tested to determine the optimum frequency. The optimum frequency in Fig. 9a varies roughly linearly with the pressure. The optimum frequency will rise together with the mechanical resonant frequency as the charge pressure increases, which is related to the increase of the stiffness of the gas spring with increasing pressure.

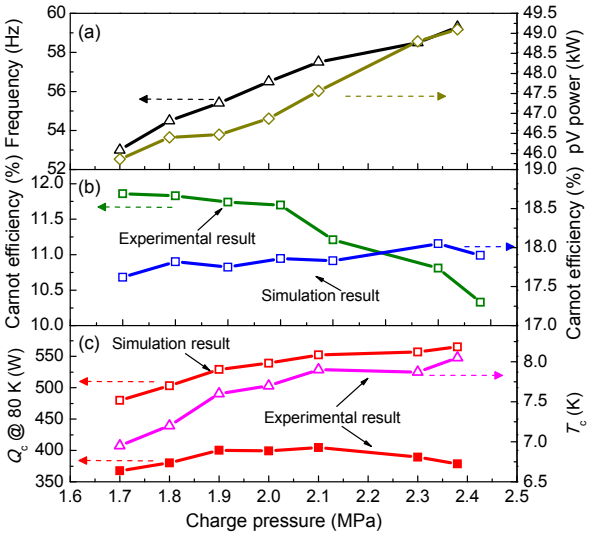

Fig. 9 Available pV power and corresponding frequency (a), relative Carnot efficiency (b), and cooling power (Q_c) at 80 K and refrigeration temperature (c) versus charge pressure from experiment and simulation with matrix 1

As shown in Fig. 9a, the no-load temperature decreases towards lower charge pressure. This is attributed to an enhanced heat transfer between the helium gas and the regenerator matrix at lower charge pressure. Nevertheless, the cryocooler cannot provide a large cooling power at lower charge pressure in spite of the lower refrigeration temperature. The reason is that a lower charge pressure results in a smaller mass flow rate which will reduce the cooling power for a given input power. On the other hand, a larger pressure leads to a higher enthalpy flow in the regenerator acting as thermal loss which degrades the cooling power. Therefore, there exists an optimum charge pressure as a compromise for achieving the best performance.

For comparison, Fig. 9c also displays the simulated cooling power at 80 K. Each point in Fig. 9c is taken at the optimum frequency as plotted in Fig. 9a. The pV power in the simulation was taken from the experimental data. The available pV power shown in Fig. 9c decreases towards lower pressure, since at lower charge pressure the stroke limit of the compressor pistons is reached at a lower pV power. As shown in Fig. 9c, the simulated cooling power increases with the increase of charge pressure because of large available pV power. However, the measured cooling power at 80 K (by linear extrapolation) does not continuously rise with charge pressure although the available pV power is larger at higher charge pressure. The optimum charge pressure from the experiment is 2.1 MPa. A comparison of the measured cooling power at 80 K with the simulation results shows a different dependence on charge pressure. Moreover, the experimental results of cooling power are between 67% and 77% of the simulation. The measured cooling power is around 112–186 W less than the simulation results. We believe this difference is caused by the losses which are not taken account in the Sage simulation, namely the temperature inhomogeneity, since it will degrade the cooling performance due to additional enthalpy loss to the regenerator (Dietrich *et al.*, 2007) and correspondingly the cooling power could be improved by reducing it with thermal conductance enhanced regenerator materials (Sun *et al.*, 2013).

The measured relative Carnot efficiency with respect to electrical input power, which is proportional to the COP, increases with decreasing charge pressure, as illustrated in Fig. 9b. This is in contrast to the calculated relative Carnot efficiency with respect to pV power. The reason is that the temperature non-uniformity in the regenerator that degrades the cooling performance goes down with decreasing pV power (mass flow). This is shown in Fig. 10, where the measured azimuthal temperature variation $\Delta T_{reg,0.5}$ (defined as the maximum difference of T_{RegA}, T_{RegB}, and T_{RegC}, see Fig. 1) is plotted as function of the pV power. Therefore, the cooling performance

suffers less from temperature non-uniformity at lower charge pressure due to less pV power consumed. That is the reason why the measured relative Carnot efficiency at lower charge pressure is higher than at the measured optimum charge pressure for cooling power. With a charge pressure of 2.1 MPa and a frequency of 57.5 Hz, the cryocooler exhibits the best performance at 80 K (Fig. 9c). Under this operating condition, the cryocooler reaches a no-load refrigeration temperature of 47.6 K, and a cooling power of 404 W at 80 K is achieved with an electrical input power of 8.9 kW.

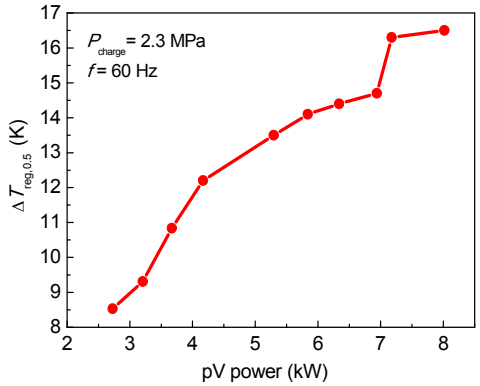

Fig. 10 Measured cooling power at 80 K versus charge pressure with matrix 2 at different input powers

Fig. 11 shows the cooling power at 80 K measured with matrix 2 as function of the charge pressure for different frequencies and input powers. For each charge pressure, the corresponding frequency shown in Fig. 11 is the optimum frequency. For each input power, there exists an optimum charge pressure with respect to maximum cooling power. Moreover, the optimum charge pressure rises with the increase of input power, as indicated by the dotted line in Fig. 10. This indicates that a higher cooling power demands a larger charge pressure.

4.3 Temperature inhomogeneity

The azimuthal temperature inhomogeneity around the circumference of the regenerator was monitored during cooler operation indicating a parasitic streaming in the regenerator (Dietrich *et al*., 2007). The performance was significantly improved by replacing some stainless steel regenerator meshes with copper or brass screens to reduce this temperature non-uniformity. Thus, it is important to investigate the dependence of temperature non-uniformity on different operating parameters in a high-power SPTC. Fig. 12 shows the azimuthal temperature variation and the no-load refrigeration temperature as function of frequency for three different charge pressures with matrix 1. The input power was kept constant at 7 kW. As seen from Fig. 12a, there exists an optimum frequency for each charge pressure corresponding to the lowest no-load refrigeration temperature. Surprisingly, in Fig. 12b the corresponding azimuthal temperature variation for the charge pressures of 1.8 and 2.0 MPa also exhibits the maximum at this optimum frequency. This may be ascribed to the fact that a lower refrigeration temperature leads to a higher temperature gradient along the regenerator and thus to a larger amount of re-circulating flow in the regenerator (Dietrich *et al*., 2007).

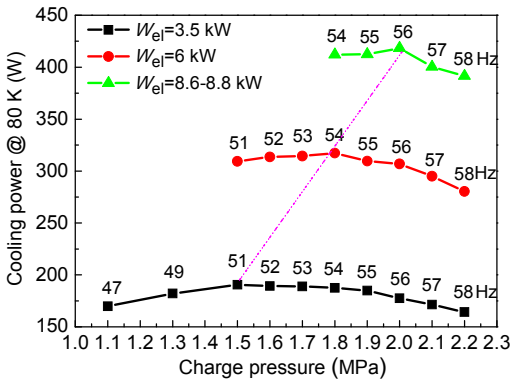

Fig. 11 Measured azimuthal temperature variation as function of pV power at 2.3 MPa and 60 Hz with matrix 2

The temperature non-uniformity is not only influenced by the temperature gradient. In addition, a higher charge pressure will increase the azimuthal temperature variation $\Delta T_{reg,0.5}$ (Fig. 12b). As a result, even though a minimum temperature is reached at 56 Hz for the pressure of 2.2 MPa, the frequency corresponding to the maximum $\Delta T_{reg,0.5}$ is 2 Hz higher. The reason is that for the pressure of 2.2 MPa the pV power conversion efficiency rises up to a maximum at 59 Hz (Fig. 8b). Given that for all three filling pressures in Fig. 12 the maximum azimuthal temperature variation is not large and relatively independent of the operating frequency, it can be concluded that the parasitic effect of the

regenerator streaming is considerably reduced by use of matrix 1.

As already seen from Fig. 10, the azimuthal temperature variation $\Delta T_{reg,0.5}$ depends strongly on pV power and therefore on input power, i.e., the more pV power (or mass flow) is generated by the compressor, the larger is the temperature non-uniformity.

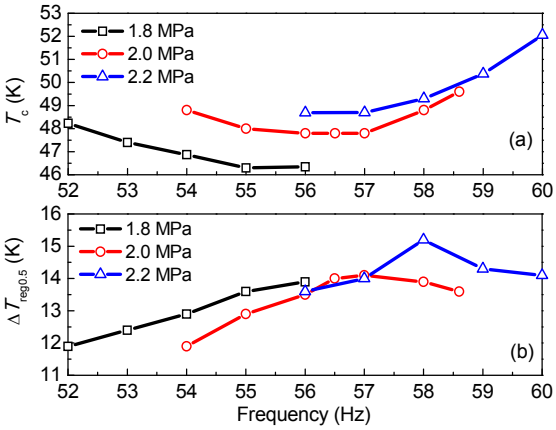

Fig. 12 Measured refrigeration temperature as function of frequency (a) and measured azimuthal temperature variation in the middle of the regenerator (matrix 1) versus frequency (b). The pV power was kept constant at 7 kW

4.4 Typical cooling performance

After optimizing the operating conditions for the highest cooling performance near 70 K, the cooling power as function of refrigeration temperature has been measured for the two matrices, as displayed in Fig. 13. At 56.5 Hz and 2.0 MPa, the minimum no-load refrigeration temperature with matrix 1 is 46.9 K, and a cooling power of 300 W at 71.8 K is obtained with an input power of 8.9 kW. The no-load refrigeration temperature with matrix 2 is roughly 5 K higher than that with matrix 1 since the temperature inhomogeneity of matrix 1 is slightly smaller than that of matrix 2 (Sun *et al.*, 2013). However, even though the matrix 1 has less thermal loss caused by temperature inhomogeneity than matrix 2, it will have more other additional losses (conduction loss for instance) compared with matrix 2. Thus, the slope of the load line with matrix 2 is 14.1 W/K compared with 12.1 W/K with matrix 1. Correspondingly the SPTC can still provide a cooling power of 299 W at 73 K with matrix 2.

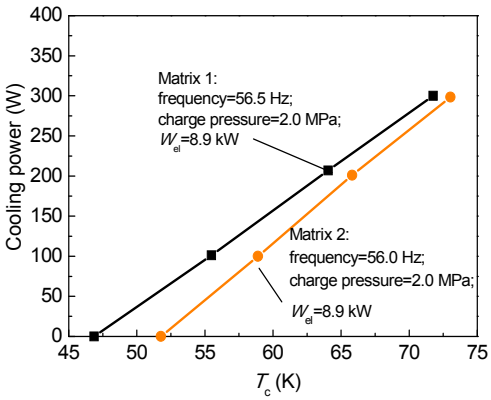

Fig. 13 Measured cooling power as function of refrigeration temperature

5 Conclusions

A high power single-stage SPTC designed for working at liquid nitrogen temperatures was theoretically and experimentally investigated. The effect of charge pressure and operating frequency on the cooling performance of the regenerator was presented. The results suggest that the frequency should be optimized to achieve the maximum compressor and regenerator efficiency. A medium charge pressure in the range of 1.9–2.1 MPa is a good compromise with respect to refrigeration temperature and enthalpy flow loss, so that a high cooling performance can be achieved.

The effect of charge pressure and operating frequency on the temperature non-uniformity in the regenerator was also analyzed. For each charge pressure, there is a certain frequency for which a maximum temperature inhomogeneity in the regenerator is reached. The temperature non-uniformity increases with the increase of input power. The optimum charge pressure also rises with increasing input power. By optimizing the working conditions, the cryocooler with matrix 1 (Fig. 6) reaches a no-load refrigeration temperature of 46.9 K when the charge pressure is 2.0 MPa and the frequency is 56.5 Hz. A cooling power of 304 W at 72 K is available at an electrical input power of 8.9 kW.

References

Dietrich, M., Thummes, G., 2010. Two-stage high frequency pulse tube cooler for refrigeration at 25 K. *Cryogenics*, **50**(4):281-286. [doi:10.1016/j.cryogenics.2010.01.010]

Dietrich, M., Yang, L.W., Thummes, G., 2007. High-power

Stirling-type pulse tube cryocooler: observation and reduction of regenerator temperature-inhomogeneities. *Cryogenics*, **47**(5-6):306-314. [doi:10.1016/j.cryogenics.2007.03.009]

Ercolani, E., Poncet, J.M., Charles, I., *et al.*, 2008. Design and prototyping of a large capacity high frequency pulse tube. *Cryogenics*, **48**(9-10):439-447. [doi:10.1016/j.cryogenics.2008.06.003]

Gan, Z.H., Liu, G.J., Wu, Y.Z., *et al.*, 2008. Study on a 5.0 W/80 K single stage Stirling type pulse tube cryocooler. *Journal of Zhejiang University-SCIENCE A*, **9**(9):1277-1282. [doi:10.1631/jzus.A0820220]

Gedeon, D., 1994. Sage: object orientated software for Stirling-type machine design. 29th Intersociety Energy Conversion and Engineering Conference. American Institute for Aeronautics Sand Astronautics, p.1902-1907.

Ghahremani, A.R., Saidi, M.H., Jahanbakhshi, R., *et al.*, 2011. Performance analysis and optimization of high capacity pulse tube refrigerator. *Cryogenics*, **51**(4):173-179. [doi:10.1016/j.cryogenics.2011.01.006]

Gromoll, B., Huber, N., Dietrich, M., *et al.*, 2006. Development of a 25 K pulse tube refrigerator for future HTS-series products in power engineering. AIP Conference Proceedings, **823**:643-652. [doi:10.1063/1.2202470]

Hu, J.Y., Zhang, L.M., Zhu, J., *et al.*, 2014. A high-efficiency coaxial pulse tube cryocooler with 500 W cooling capacity at 80 K. *Cryogenics*, **62**:7-10. [doi:10.1016/j.cryogenics.2014.03.010]

Imura, J., Iwata, N., Yamamoto, H., *et al.*, 2008. Optimization of regenerator in high capacity Stirling type pulse tube cryocooler. *Physica C: Superconductivity*, **468**(15-20):2178-2180. [doi:10.1016/j.physc.2008.05.281]

Potratz, S.A., Abbott, T.D., Johnson, M.C., *et al.*, 2008. Stirling-type pulse tube cryocooler with 1 kW of refrigeration at 77 K. AIP Conference Proceedings, **985**:42-48. [doi:10.1063/1.2908581]

Sun, D.M., Dietrich, M., Thummes, G., 2009a. High-power Stirling-type pulse tube cooler working below 30 K. *Cryogenics*, **49**(9):457-462. [doi:10.1016/j.cryogenics.2009.06.006]

Sun, D.M., Dietrich, M., Thummes, G., *et al.*, 2009b. Investigation on regenerator temperature inhomogeneity in Stirling-type pulse tube cooler. *Chinese Science Bulletin*, **54**:986-991. [doi:10.1007/s11434-009-0123-5]

Sun, J.C., Qiu, L.M., Thummes, G., *et al.*, 2013. Experimental investigation of hybrid regenerator fillings with high thermal conductance in high power pulse tube cryocoolers. *Journal of Engineering Thermophysics*, **34**:605-608 (in Chinese).

Wakeland, R.S., 2000. Use of electrodynamic drivers in thermoacoustic refrigerators. *Journal of the Acoustical Society of America*, **107**:827-832. [doi:10.1121/1.428265]

Yan, P.D., Gao, W.L., Chen, G.B., 2009. Development of a linear compressor for two-stage pulse tube cryocoolers. *Journal of Zhejiang University-SCIENCE A*, **10**:1595-1600. [doi:10.1631/jzus.A0820742]

中文概要

题　目：液氮温区单级大功率斯特林型脉管制冷机工作特性研究

目　的：探索充气压和运行频率等工作特性对大功率脉管制冷机最低制冷温度、制冷量以及回热器温度不均匀性的影响，期望进一步提升制冷机工作性能。

方　法：1. 通过理论计算模拟工作频率在 40–70 Hz，充气压力在 1.5–2.5 MPa 下工作特性对制冷机性能的影响；2. 实验研究充气压力为 1.7–2.4 MPa，并在谐振频率附近工作时制冷机性能以及回热器温度不均匀性随充气压力、运行频率以及输入功率的变化。

结　论：1. 制冷机运行在 1.9–2.1 MPa 充气压力下，因平衡了制冷温度和焓流损失，故能取得优异性能，且每一个充气压力对应一个最优的工作频率；2. 通过优化充气压力和工作频率，脉管制冷机能够达到 46.9 K 的最低制冷温度，此时工作频率为 56.5 Hz，充气压力为 2.0 MPa。在 8.9 kW 输入功率下制冷机能够在 72 K 时提供 304 W 制冷量。

关键词：斯特林型脉管制冷机；大功率；工作特性；温度不均匀性